Ultrafast all-optical switching and error-free 10 Gbit/s wavelength conversion in hybrid InP-silicon on insulator nanocavities using surface quantum wells

Alexandre Bazin, Kevin Lenglé, Mathilde Gay, Paul Monnier, Laurent Bramerie, Remy Braive, Grégoire Beaudoin, Isabelle Sagnes, Rama Raj, Fabrice Raineri

Ultrafast all-optical switching and error-free 10 Gbit/s wavelength conversion in hybrid InP-silicon on insulator nanocavities using surface quantum wells

Alexandre Bazin,[1] Kevin Lenglé,[2,3] Mathilde Gay,[2,3] Paul Monnier,[1] Laurent Bramerie,[2,3] Rémy Braive,[1,4] Grégoire Beaudoin,[1] Isabelle Sagnes,[1] Rama Raj,[1] and Fabrice Raineri[1,4,a)]

[1]*Laboratoire de Photonique et de Nanostructures (CNRS UPR20), Route de Nozay, Marcoussis 91460, France*
[2]*Université Européenne de Bretagne (UEB), 5 Boulevard Laënnec, 35000 Rennes, France*
[3]*CNRS-Foton Laboratory (UMR 6082), Enssat, BP 80518, 22305 Lannion Cedex, France*
[4]*Université Paris Diderot, Sorbonne Paris Cité, 75207 Paris Cedex 13, France*

(Received 21 October 2013; accepted 18 December 2013; published online 2 January 2014)

Ultrafast switching with low energies is demonstrated using InP photonic crystal nanocavities embedding InGaAs surface quantum wells heterogeneously integrated to a silicon on insulator waveguide circuitry. Thanks to the engineered enhancement of surface non radiative recombination of carriers, switching time is obtained to be as fast as 10 ps. These hybrid nanostructures are shown to be capable of achieving systems level performance by demonstrating error free wavelength conversion at 10 Gbit/s with 6 mW switching powers. © *2014 AIP Publishing LLC*.
[http://dx.doi.org/10.1063/1.4861121]

Ultrafast all-optical switching is one of the key functionalities in an optical network to process information by routing, gating, converting, etc., data at high bit rates. Recently, the drive towards the miniaturisation and the energy efficiency of such switches motivated important efforts in research especially in the nanophotonics domain. In this context, Photonic crystal (PhC) high-Q cavities[1,2] showed their capacity to provide both footprints $<50\ \mu m^2$ and high nonlinear response with few fJ activation energies.[3] However, the operation of these devices at high bit rates in system experiments, is still missing. This can be explained by the use of material systems which do not enable a fast switch recovery. Indeed, to build all-optical switches, carrier induced change in refractive index due to photo-excitation is widely used, giving a switching dynamics directly governed by the carrier lifetime. GaAs-based PhC-based switches show extremely fast response with 8 ps[4–6] recovery times due to dominant non radiative recombination of carriers but with switching energies higher than 100 fJ (Ref. 5) and with inherent oxidation problems. The best results were obtained using InP-based PhC nanocavities[3] which allowed sub-fJ operation with a partly fast (20 ps) carrier recombination process linked to their diffusion out of the small cavities but with a longer component lasting over 200 ps which is not adapted for bit rates beyond 5 Gbits/s. Further, operating all-optical switches at high bit rates require a mastery over heat sinking, as thermal effects cause a refractive index change, which counteract the one induced by carrier injection and may cause irreversible damage to the structure. This is particularly true for ultra compact devices based on PhC membranes as they are usually suspended in air which prevents heat evacuation.

In this letter, we report the judicious combination of the manipulation of the carrier lifetime in InP-based materials through surface growth of quantum wells (QWs) and material processing so as to maximise the speed of the nonlinear response with a view to obtaining high speed all-optical PhC switches. The III-V semiconductors PhC cavities are integrated onto Silicon on Insulator (SOI) waveguides which permits an efficient interfacing of the switches with the external world as well as to envision complex complementary metal oxide semiconductor (CMOS) compatible circuits, incorporating active and passive devices.[7] Switching time of 10 ps and activation energy of 40 fJ are measured. We demonstrate in a system experiment that these features enable error-free wavelength conversion at 10 Gbits/s.

Several approaches have been explored for reducing the carrier lifetime, such as carrier diffusion,[8] low temperature growth,[9] stimulated recombination of carriers,[10] ion implantation,[11,12] carrier sweeping[13] or surface recombination.[14] In particular, in planar PhCs, the carrier lifetime is strongly affected by surface recombination at the walls of the etched holes.[15] Indeed, the typical patterning dimensions of these structures (∼100 nm) are well below the diffusion length of the carriers which results in a decrease of the carrier lifetime, from nanoseconds to 200 ps in InP-based material.[10] Further, it is possible to reduce even more the lifetime of the carriers by material engineering as using surface growth of QWs.[14]

The hybrid PhC structure under investigation is shown in Fig. 1(a). A 260 nm thick InP slab is flanked by a single 10 nm QW on both sides. The absorption edge of the InGaAs QWs is chosen to be near 1.55 μm. The SOI waveguides are patterned using DUV lithography on a CMOS line. The 220 nm thick Si layer is entirely etched, leaving waveguides on SiO_2 of widths from 250 nm to 550 nm. At the extremities of each waveguide, shallow grating couplers are etched for inputting and outputting light. The InP slab is bonded onto the SOI die using benzocyclobutene[16] (BCB). The BCB layer spun is 300 nm thick so that only 80 nm of the polymer is above the SOI wire. Prior to the bonding, the InP slab is coated with a 300 nm thick SiO_2 layer in order to put the SOI level and the III-V PhC level at the desired distance.

This combination of the ultrathin BCB bonding layer with the SiO_2 layer results in an improved heat sinking of the

a)E-mail: fabrice.raineri@lpn.cnrs.fr

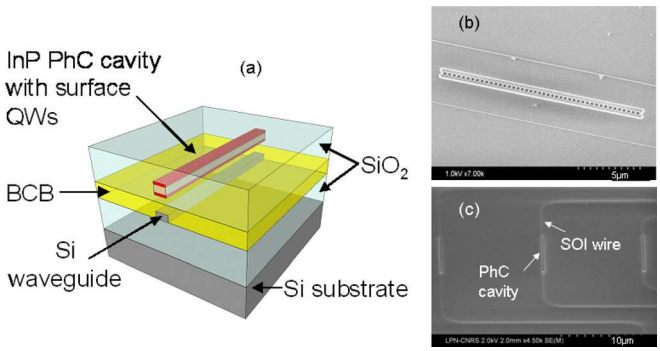

FIG. 1. (a) Schematics of the hybrid structure. (b) SEM picture of the InP-based PhC nanobeam cavity before SiO_2 encapsulation. (c) SEM picture of the InP-based PhC nanobeam cavity aligned to the SOI waveguides.

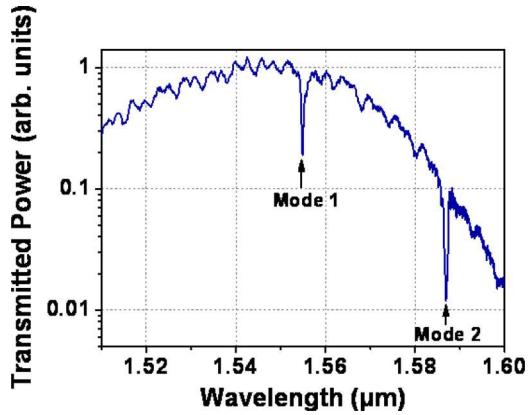

FIG. 2. Measured transmission of the evanescently coupled hybrid InP on SOI system loaded with the surface QWs absorption.

InP-based PhC and an improved control over the evanescent wave coupling between the two optical levels. The sample is then fully encapsulated in SiO_2 to increase further heat evacuation.

We then designed and fabricated PhC nanobeam cavities consisting of a row of equally sized holes drilled into a semiconductor single mode waveguide. The distance between the holes is subtly varied[17] in order to obtain a Gaussian apodisation[18] of the electromagnetic field profile which enables quality factors greater than 10^6 in modal volumes of the order $(\lambda/n)^3$ for cavities fully embedded in SiO_2. Not only do these cavities have a small footprint of 10 μm^2, their design also offers an ease in the technological processing as only the period is changed and the size of the holes remains the same.

The InP based QW heterostructure is processed to obtain a nanobeam waveguide (650 nm × 280 nm) with a single row of holes (targeted radius r = 120 nm) drilled to form the PhC cavity using electron beam lithography followed by plasma etching. Care is taken to optimally align the photonic cavity and the silicon waveguide in order to ensure good evanescent wave coupling.[19]

SEM pictures of the fabricated structures are shown in Figs. 1(b) and 1(c). To tune the resonant wavelength around 1550 nm, the lattice constant, a_0, in the central part of the cavity is varied between 340 nm and 365 nm in steps of 2.5 nm.

A transmission spectrum measured through a 350 nm wide SOI waveguide coupled to a PhC nanobeam cavity ($a_0 = 357.5$ nm) is shown in Fig. 2. The resonant modes are visible as dips in the transmission, at 1554.7 nm and 1586.9 nm. The associated Q factors are, respectively, 1720 and 1250. These Q factors correspond to that of the cavity loaded with the coupling to the SOI waveguide and with the absorption of the QWs. From coupled mode theory,[7] one can calculate the transmission at resonance as a function of the Q factor of the unloaded cavity (Q_0), and the Q factors associated with the coupling to the waveguide (Q_c) and with the losses due to material absorption (Q_{abs}). It writes

$$T = \left(1 - \frac{\frac{1}{Q_c}}{\frac{1}{Q_0} + \frac{1}{Q_c} + \frac{1}{Q_{abs}}}\right)^2.$$

Thus, we can infer for mode 1, $Q_c = 3100$ and for mode 2, $Q_c = 1800$.

As shown in Ref. 7, Q_c can be tuned by choosing the appropriate width of the waveguide with a direct impact on the depth of the dip and on the expected switching contrast. Q_{abs} is experimentally deduced by saturating the absorption using ps pulses and measuring the transmission spectrum. At 1550 nm, Q_{abs} is equal to 5000. This gives for mode 1 $Q_0 = 17000$. As for mode 2, Q_{abs} at 1580 nm expected to be higher than at 1550 nm could not be measured due the limited tuning range of our ps source. Note, here, we chose to work with relatively low values of Q in order to not be limited by the photon lifetime in our cavity-based switches.

In order to demonstrate the capacity of this system to be used as a fast and efficient switch, we perform non-degenerate as well as degenerate pump-probe experiments. The first uses, as pump, a Ti:Saph laser focused on the surface of the cavity, delivering 100 fs pulses at 80 MHz at 800 nm. It excites carriers both in the QWs and in the InP slab. An optical parametric oscillator (OPO) which may be tuned between 1500 nm and 1590 nm delivering 100 fs pulses too at 80 MHz (pumped by the Ti:Saph) is used as a probe. The probe pulses are spectrally 25 nm broad, so the resonance spectrum is measured in one shot. As the pump-probe delay (Δt) is varied, the carrier level is probed by the wavelength shift of the resonance within the transmission of the OPO pulse spectrum.

The spectrum of the probe pulses transmitted through the sample is plotted in Fig. 3(a) as a function of Δt, for an absorbed pump energy of 6 fJ. When the probe arrives before the pump (negative Δt), the cold cavity seen by the probe gives a dip in the transmission situated at $\lambda_0 = 1554.7$ nm. Immediately after the arrival of the pump, we can see that the resonance blue-shifts by $\Delta\lambda_{max} = 1.8$ nm due to the associated rise in the carrier density in the semiconductor (rise time ~ 0.9 ps). This is accompanied by a narrowing of the resonance because of the absorption bleaching of the QWs, which attests to an increase of the loaded Q factor up to 11 000. Then, as the pump-probe delay is increased, the resonance gradually shifts and widens back to its initial wavelength and linewidth due to the recombination of the carriers. To extract the carrier lifetime, we plot in Fig. 3(b) the resonant wavelength as a function of Δt and fit the

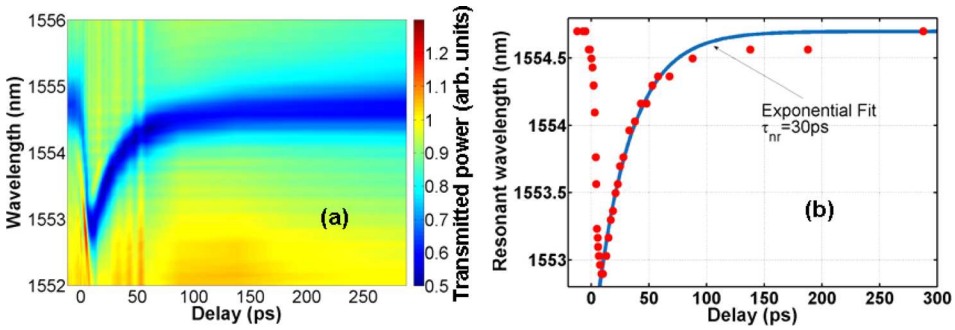

FIG. 3. (a) Spectrum of the transmitted probe as a function of the pump-probe delay. (b) Resonant wavelength as a function of the pump-probe delay (red dots).

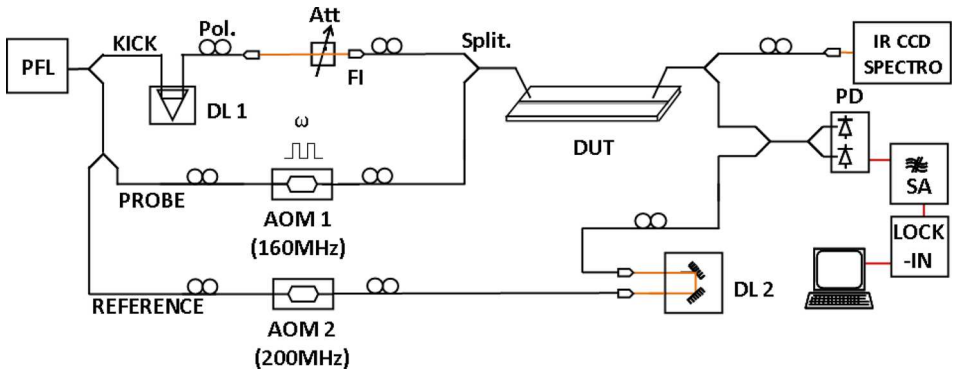

FIG. 4. Degenerate pump-probe experiment set-up with heterodyne detection. PFL: Picosecond fibre laser. Pol: Polarizer. DL: Delay line. Att: Attenuator. FI: Fibre injector. Split: 50/50 fibre splitter. AOM: Acousto-optic modulator. IR SPECTRO: Spectrometer equipped with a cooled array of InGaAs detectors. PD: Balanced photodetectors. SA: Electrical spectral analyser.

obtained experimental data with a single exponential function (represented by the continuous curve) which writes

$$\lambda(\Delta t) = \lambda_0\left(1 - \frac{\Delta\lambda_{\max}}{\lambda_0}\exp\left(\frac{-\Delta t}{\tau_{nr}}\right)\right),$$

where τ_{nr} is the carrier decay time. We find that the exponential function fits closely the experiment for τ_{nr} equal to 30 ps. This indicates that the carrier lifetime is entirely determined by the non radiative recombination processes which are here greatly enhanced by the deliberate manipulation of the material. This fast return of the carrier gives a first estimation of the speed (~30 GHz) of operation of a switch based on this type of sample. To determine accurately the switching speed, it is necessary to perform a pump probe experiments where the probe pulse bandwidth is of the order of the resonance linewidth of the cavity as it is in this configuration that the system should be operated to obtain maximum switching contrast. Degenerate pump-probe experiment using a heterodyne detection scheme[20] (depicted in Fig. 4), is carried out to measure the switching speed.

The source used for this experiment is a mode-locked fibre laser which provides 2 ps long pulses at a 22 MHz repetition rate which match the cavity bandwidth. The source wavelength is set on resonance (low transmission). The probe is discriminated from the pump by detecting in the balanced detectors a harmonic of the probe/reference beat note, here at 4 MHz. This signal is filtered using an electrical spectrum analyser and is recorded using a lock-in amplifier set at $\omega = 2$ kHz. We plot in Fig. 5, the measured probe transmission normalized to its peak value as a function of the pump-probe delay.

Right after the pump pulses arrival, the probe transmission rapidly jumps to its peak value as the resonance shifts away from the probe wavelength. When the pump pulses energy is set at 40 fJ (inside the SOI waveguide), a contrast greater than 50% is obtained in the probe transmission. Here, the pump pulses are only absorbed within the InGaAs surface QWs and not in the InP slab. As the pump-probe delay is increased, the system returns to its equilibrium state leading to a decrease in the probe transmission. An exponential fit of the return of the probe transmission to its initial value gives a switching time of 10 ps, 3 times faster than the carrier lifetime letting us envisage switching experiments on high bit rate data stream.

High-bit rate operation of these devices is demonstrated by performing wavelength conversion in the conditions of a system experiment using non-return-to-zero (NRZ) encoded signals. A 10 Gbit/s pseudorandom binary sequence is injected at Mode 2 wavelength (see Fig. 2) as a pump signal. A continuous probe signal is sent into Mode 1. When the

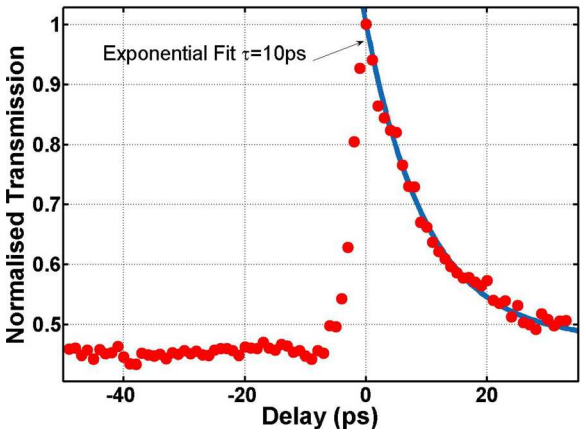

FIG. 5. Normalised probe transmission versus pump-probe delay for 40 fJ pump energy.

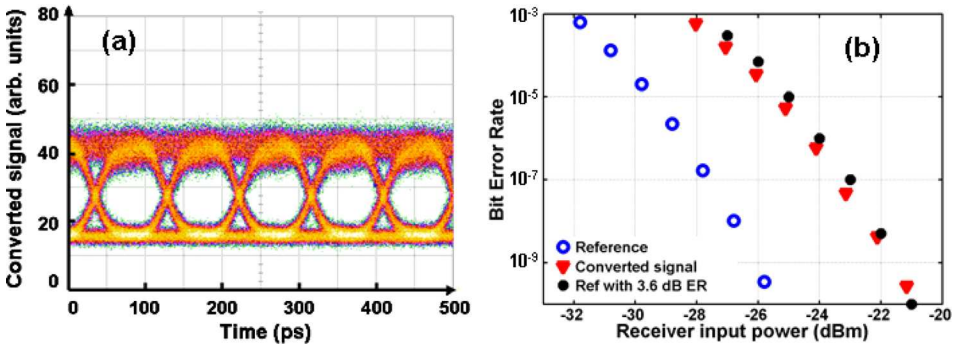

FIG. 6. (a) Eye diagram of the NRZ wavelength converted signal at 10 Gbit/s. (b) Measured bit error rate at 10 Gbit/s versus the receiver input power for the reference (blue circles) and for the converted signal (red triangles). The black dots indicate the bit error rate of the reference with a degraded ER of 3.6 dB.

cavity resonance shifts dynamically under the pump action (here of about 0.5 nm), the probe transmission increases converting thereby the signal at the probe wavelength. For a pump coupled peak power of 6 mW, a fully open converted eye diagram with no signal distortion is obtained (see Fig. 6(a)). As indicated in Fig 6(b), the bit error rate (BER) measurements show error free operation on the converted signal (red triangles) with a power penalty of 4 dB compared to the reference.

To evaluate the origin of this penalty, we artificially degrade the extinction ratio (ER) of the reference signal to the extinction ratio of the degraded signal (3.6 dB) by adjusting the bias voltage of the modulator. Result is plotted with black dots in Fig. 6(b) showing a good agreement with the wavelength converted curve. We can thus conclude that the low ER of the converted signal is at the origin of the BER degradation and that the time response of the device has no impact on the BER at this bit rate. This clearly demonstrates that the BER is not limited by the dynamics of the switching mechanism provided by our hybrid InP/SOI PhC cavities with InGaAs surface QWs.

In conclusion, we have demonstrated that InP PhC nanocavities with InGaAs surface QWs incorporated in a III-V/SOI hybrid platform, constitute an efficient system for achieving ultrafast switches activated with low energies. We have showed that the recovery time of these all-optical switches can be as fast as 10 ps thanks to the enhancement of the non radiative surface recombination rate of carriers, and that the activation energies can be as low as few tens of fJ. We have also proved that these hybrid PhCs are capable of achieving systems level performance by demonstrating error free wavelength conversion at 10 Gbit/s. This result makes evident the huge possibilities of III-V/SOI nanophotonics which combines the versatility and the efficiency of III-V semiconductors to provide active functionalities such as ultrafast switching and emission with the capacity of SOI waveguides circuitry to channel the optical information throughout an optical chip.

We acknowledge the FP7 European Project COPERNICUS as well as the French ANR jeunes chercheurs PROWOC.

[1]Y. Akahane, T. Asano, B. S. Song, and S. Noda, Nature **425**, 944 (2003).
[2]E. Kuramochi, M. Notomi, S. Mitsugi, A. Shinya, T. Tanabe, and T. Watanabe, Appl. Phys. Lett. **88**, 041112 (2006).
[3]K. Nozaki, T. Tanabe, A. Shinya, S. Matsuo, T. Sato, H. Taniyama, and M. Notomi, Nature Photon. **6**, 248 (2012).
[4]A. M. Yacomotti, F. Raineri, G. Vecchi, I. Sagnes, M. Strassner, L. Le Gratiet, R. Raj, and A. Levenson, Appl. Phys. B **81**, 333–336 (2005).
[5]C. Husko, A. De Rossi, S. Combrié, Q. V. Tran, F. Raineri, and C. W. Wong, Appl. Phys. Lett. **94**, 021111 (2009).
[6]A. D. Bristow, J.-P. R. Wells, W. H. Fan, A. M. Fox, M. S. Skolnick, D. M. Whittaker, A. Tahraoui, T. F. Krauss, and J. S. Roberts, Appl. Phys. Lett. **83**, 851 (2003).
[7]Y. Halioua, A. Bazin, P. Monnier, T. J. Karle, G. Roelkens, I. Sagnes, R. Raj, and F. Raineri, Opt. Express **19**, 9221–9231 (2011).
[8]T. Tanabe, H. Taniyama, and M. Notomi, J. Lightwave Technol. **26**, 1396–1403 (2008).
[9]I. Lahiri, D. Nolte, E. Harmon, M. Melloch, and J. Woodall, Appl. Phys. Lett. **66**, 2519 (1995).
[10]F. Raineri, C. Cojocaru, P. Monnier, A. Levenson, R. Raj, C. Seassal, X. Letartre, and P. Viktorovitch, Appl. Phys. Lett. **85**, 1880 (2004).
[11]E. Lugagne Delpon, J. L. Oudar, N. Bouché, R. Raj, A. Shen, N. Stelmakh, and J. M. Lourtioz, Appl. Phys. Lett. **72**, 759 (1998).
[12]T. Tanabe, K. Nishiguchi, A. Shinya, E. Kuramochi, H. Inokawa, M. Notomi, K. Yamada, T. Tsuchizawa, T. Watanabe, H. Fukuda, H. Shinojima, and S. Itabashi, Appl. Phys. Lett. **90**, 031115 (2007).
[13]S. F. Preble, Q. Xu, B. S. Schmidt, and M. Lipson, Opt. Lett. **30**, 2891–2893 (2005).
[14]C. Symonds, J. Mangeney, G. Saint-Girons, and I. Sagnes, Appl. Phys. Lett. **87**, 012107 (2005).
[15]K. Tai, T. R. Hayes, S. L. McCall, and W. T. Tsang, Appl. Phys. Lett. **53**, 302 (1988).
[16]G. Roelkens, J. Brouckaert, D. Van Thourhout, R. Baets, R. Notzel, and M. Smith, J. Electrochem. Soc. **153**, G1015 (2006).
[17]A. Bazin, R. Raj, and F. Raineri, "Design of silica encapsulated high-Q photonic crystal nanobeam cavities," IEEE J. Lightwave Technol. (preprint)
[18]Y. Tanaka, T. Asano, and S. Noda, J. Lightwave Technol. **26**, 1532 (2008).
[19]T. J. Karle, Y. Halioua, F. Raineri, P. Monnier, R. Braive, L. Le Gratiet, G. Beaudoin, I. Sagnes, G. Roelkens, F. van Laere, D. Van Thourhout, and R. Raj, J. Appl. Phys. **107**, 063103 (2010).
[20]A. Mecozzi and J. Mørk, J. Opt. Soc. Am. B **13**, 2437–2452 (1996).